Heat exchanger fouling & cleaning conference 2019
Analysis of crystallization fouling durability of novel heating elements for electric water heating

ANALYSIS OF CRYSTALLIZATION FOULING DURABILITY OF NOVEL HEATING ELEMENTS FOR ELECTRIC WATER HEATING

A. Janzen[1] and E. Y. Kenig[2,3]
[1] Stiebel Eltron GmbH & Co. KG, Dr.-Stiebel-Straße 33, 37603 Holzminden, Germany,
E-mail: alexander.janzen@stiebel-eltron.de (corresponding author)
[2] Chair of Fluid Process Engineering, University of Paderborn, Pohlweg 55, 33098 Paderborn, Germany
[3] Gubkin Russian State University of Oil and Gas, Moscow, Russian Federation

ABSTRACT

New materials and technologies offer the means to develop novel electrical heating systems with improved durability against crystallization fouling. In this study, an analysis of both conventional and novel heating elements under the influence of crystallization fouling is presented. The novel heating elements are based on two different coating technologies, namely, thermal spraying and thin film sputtering. The novel heating elements reach heat fluxes exceeding 15 W/cm² and an electrical power of approximately 1000 W. All presented heating elements operate under clean surface conditions for approximately 1000 h without any difficulties. Different properties of the presented heating elements result in different types of fouling behavior. The duration tests also demonstrate different fouling durability, which results in different lifetimes. Furthermore, it is shown that the electrical resistance of the heating conductor is adversely affected by the fouling. A comparison shows that all novel electric heating elements exhibit longer lifetimes than tubular heating elements.

INTRODUCTION

Electric water heating

Electrical heating appliances have been used for many years in water heating. There are primarily two heating systems manufactured in large quantities, which are based either on tubular or bare-wire heating elements. The tubular heating element is an electrical resistance heater in a sheath made of copper, stainless steel, or steel. A heating wire is embedded inside the metal tube and electrically insulated with highly compressed magnesium oxide. The heating fluid has no contact with the heating wire. Owing to the poor thermal conductivity of magnesium oxide, the surface temperature of the heating wire increases. Because it is highly susceptible to crystalline deposits, its lifetime is limited. Tubular heating elements are not affected by air dissolved in water and are suitable for soft water conditions. Bare-wire heating elements operate in an electrically insulated block. Inside the block, the electric heating elements are placed directly in the fluid without any electrical insulation of the heating surface from the fluid. Insulation resistance is ensured by long and narrow channels in front of and behind the electric heating elements. This resistance depends on the properties of the fluid flowing through the long and narrow channels, and the channel geometry. Fig. 1 shows some conventional electric heating elements.

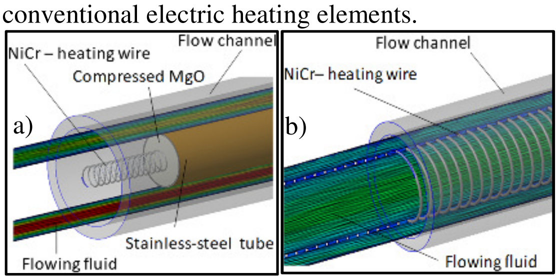

Fig. 1. Schematic of the conventional electric heating elements: tubular heating element (a); bare-wire heating element (b)

Bare-wire heating elements are especially suitable for use in hard water conditions, because they have lower surface temperature at similar operating conditions, compared to that of conventional tubular heating elements. Gusig and Schmitz [1] summarize advantages and disadvantages of conventional electric heating systems, which are shown in Table 1.

Table 1. Advantages and disadvantages of heating systems

Bare-wire heating systems	Tubular heating systems
Advantages	
Low surface temperature	No electrical contact with the fluid
Fast cooling because of low thermal mass	Low-pressure loss
Disadvantages	
Direct electrical contact with the fluid	High surface temperature
High-pressure loss because of long and narrow channels	Slow cooling because of high thermal mass

Electric heating elements have different technical properties regarding their heat transfer and, thus,

ISBN: 978-0-9984188-1-0; Published online www.heatexchanger-fouling.com

their fouling behavior. Furthermore, knowledge of the fouling behavior of electric heating elements is limited. Such knowledge is necessary for the successful development of design principles for novel heating-element generation. Therefore, novel heating elements, based on two different coating technologies, are presented, which should eliminate the disadvantages of conventional heating elements.

Electrical resistance heating

All metals and special ceramic types (e.g., titanium suboxide (TiO_x), nickel-chromium (NiCr), tin oxide (SnO)) conduct electricity. When an electrical current flows through such a material having a certain resistance, it generates heat. The power generated by the resistance can be determined with the following equation:

$$P_{el} = U_{el} \cdot I_{el} = I_{el}^2 \cdot R_{el} = \frac{U_{el}^2}{R_{el}} \qquad (1)$$

where P_{el} is the power in watts, U_{el} is the voltage across the element, I_{el} is the current through the element, and R_{el} is the electrical resistance of the element. The resistance of a given element is directly proportional to its length l and inversely proportional to its cross-sectional area A. The resistivity ρ_{el} depends on the material of the element, rather than its geometry. The following equation expresses this relationship:

$$R_{el} = \frac{U_{el}}{I_{el}} = \frac{\rho_{el} \cdot l}{A} \qquad (2)$$

The temperature dependence of electrical resistance and, thus, of electric heating devices has to be considered when constructing electrical heating systems. Normally, a dimensionless ratio R_{el}^*, which describes the resistance behavior at the temperature of the device related to the resistance at the ambient temperature of 25 °C, is considered. Equation (3) shows the normalized electrical resistance R_{el}^*:

$$R_{el}^* = \frac{R_{el}(T)}{R_{el}(T_{am})}. \qquad (3)$$

Electrical resistances primarily have two types of temperature behavior. A positive temperature coefficient (PTC) refers to materials that experience an increase in electrical resistance when their temperature is raised, while a negative temperature coefficient (NTC) refers to materials that experience a decrease in electrical resistance when their temperature is raised. In this study, both types of behavior are observed during the operation of heating conductors, as shown in Fig. 2. The figure shows the temperature dependence of normalized electrical resistance for various heating conductors.

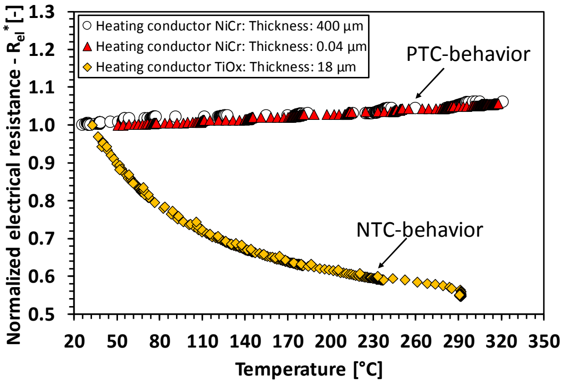

Fig. 2. The temperature dependence of normalized electrical resistance for different heating conductors

Coating technologies

The novel heating elements are based on two coating technologies, namely, thermal spraying and thin film sputtering. Thermal spraying techniques are coating processes in which melted materials are sprayed onto a surface. The coating precursor is heated by electricity or plasma. In the plasma spraying process, the material to be deposited—the feedstock—is typically a powder, liquid, suspension, or wire. It is introduced into the plasma jet, where the material is melted and propelled toward a substrate. There, the molten droplets flatten, rapidly solidify, and form a deposit. Commonly, the deposits remain adherent to the substrate as coatings, free-standing parts that can also be produced by removing the substrate. In this study, we consider thermally sprayed multilayer coating systems containing electrically insulating and conductive materials. In [2] and [3], novel ceramic heating elements are presented, produced by the thermal spraying process. These heating elements are utilized for the heating of components, machines, and machining tools, with a stability duration exceeding 300 h.

Sputter deposition is a physical vapor deposition (PVD) method that involves thin film deposition through the sputtering process. This involves a plasma jet approaching an ejecting material (the so-called target) which, in turn, emits material ions onto a substrate, as discussed in [4]. The sputtered ions can fly ballistically from the target in straight lines and impact energetically on the substrates. Sputtering is one of the main processes of manufacturing optical waveguides [5]. Furthermore, thin film heaters are widely used in various fields of electronics and microelectronics applications, which are manufactured by physical vapor deposition and chemical vapor deposition processes, as presented in [6] and [7]. Both coating technologies provide new possibilities for use of electrically insulated and conducted coating layers to develop electric heating elements that have better properties than conventional heating elements.

Crystallization fouling

Fouling is the unwanted forming of deposits on technically used surfaces. Different technical surfaces (e.g., materials) exhibit different fouling behavior owing to the different mechanical and energetic interactions on the interface between the surface and fluid, as discussed by Förster et al. [10]. Furthermore, fouling can cause severe damage to the heating devices, as shown in several investigations [8-12]. In the electric water heating, it is necessary to change the entire heating system when the heating elements fail to make the device operational again. As a result of fouling, the operation and maintenance costs of water heating increase significantly. By decreasing the fouling in heat exchangers, harmful environmental and economic effects can be reduced, as explained by Müller-Steinhagen [11].

To determine the fouling behavior, the thermal fouling resistance R_f is determined based on the reciprocal of the overall heat transfer coefficients of the clean and soiled surfaces as follows:

$$R_f = \frac{1}{k_f} - \frac{1}{k_0} \tag{4}$$

where k_f is the overall heat transfer coefficient for the fouling case and k_0 is the overall heat transfer coefficient for the initial clean condition. The overall heat transfer coefficients k_f under fouled conditions are calculated based on the temperature difference between the heating element surface $T_{s,f}$ and the fluid T_{fl}:

$$k_f = \frac{\dot{q}_{el,f}}{T_{s,f} - T_{fl}} \tag{5}$$

Fig. 3 shows a typical fouling curve. The characteristic fouling process is subdivided into two successive fouling stages: the induction period and the layer growth period.

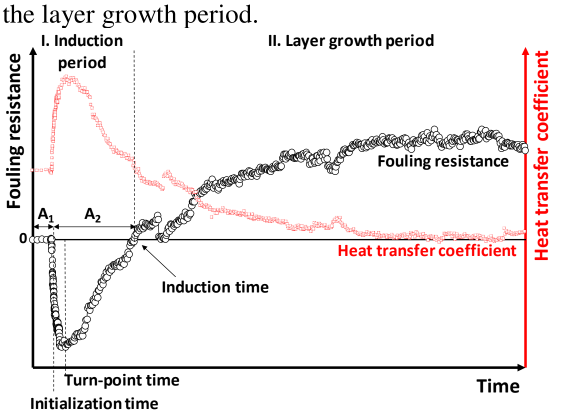

Fig. 3. Characteristic fouling curve for a $CaCO_3$ solution: A_1: Initialization phase; A_2: Roughness-controlled phase

The induction period is further separated into the initialization phase (A_1) and roughness-controlled phase (A_2). The induction period is described by the initialization time, turn-point time, and induction time. An induction period is visible in many yet not all cases. In most cases, no degradation of heat transfer is observed during this period. The initialization time describes the start of nucleation and crystal growth. After this time, the heat transfer coefficient increases at a greater rate than the heat conduction resistance. The turn-point time corresponds to the maximum heat transfer coefficient. After this time, the heat transfer coefficient slowly decreases, and the heat conduction resistance continuously increases. The induction time determines the end of the induction period. This is followed by the layer growth period, which is accompanied by a reduction in the heat transfer coefficient. The temporal evolution of the fouling process may take various forms. A distinction is made between exponential, linear, continuously increasing, asymptotic, and saw-tooth behavior. The driving power for crystallization fouling is the level of supersaturation at the heating surface that can be expressed by the saturation index, as reported by Wisotzky [13]. The saturation index is the common logarithm of the ratio of the actual ionic activity product IAP to the solubility product K_L, as follows:

$$SI = log\left(\frac{IAP}{K_L}\right) \tag{6}$$

The tap water solution at the heating surface must be supersaturated, i.e., the saturation index must be greater than zero for crystallization fouling [13].

EXPERIMENTAL

Fouling experiments

In contrast to other studies, e.g., [8-12], the fouling tests were conducted in a contaminated fluid. For tap water and ground water, the level of supersaturation can be descripted with the saturation index (Eq. 6). The saturation indices are calculated with the commercial hydrogeochemical calculation program PHREEQC [14]. To determine the saturation index and the influence of the test fluid, a tap water sample was taken before and after each test, followed by tap water analysis. A total of 60 tap water analyses were evaluated, and the arithmetic mean was used as a reference value for the different tap water components. Table 2 contains the data obtained from the tap water analysis.

Table 2. Results of tap water analysis

Property / component	Unit	Value
Temperature	[°C]	12.5
pH value	[-]	7.4
Electrical conductivity	[µS/cm, 25 °C]	897.4
Oxygen	[mmol/l]	0.1
Total hardness	[°dH]	29.2
Carbonate hardness	[°dH]	15.0
Hydrogen carbonate	[mmol/l]	5.4
Chloride	[mmol/l]	0.5
Sulfate	[mmol/l]	2.2
Nitrate	[mmol/l]	0.1
Calcium	[mmol/l]	3.0
Magnesium	[mmol/l]	2.4
Sodium	[mmol/l]	0.2
SI Aragonite	[-]	0.13
SI Aragonite, T_f = 60 °C	[-]	0.71

An experimental set-up was designed to study the characteristics of crystallization fouling for different heating elements, as illustrated in Fig. 4. Furthermore, this experimental set-up was also used to conduct duration tests under clean surface conditions. This procedure is necessary to check that the novel electric heating elements and their multifunctional coatings adhere to the electric water heating requirements.

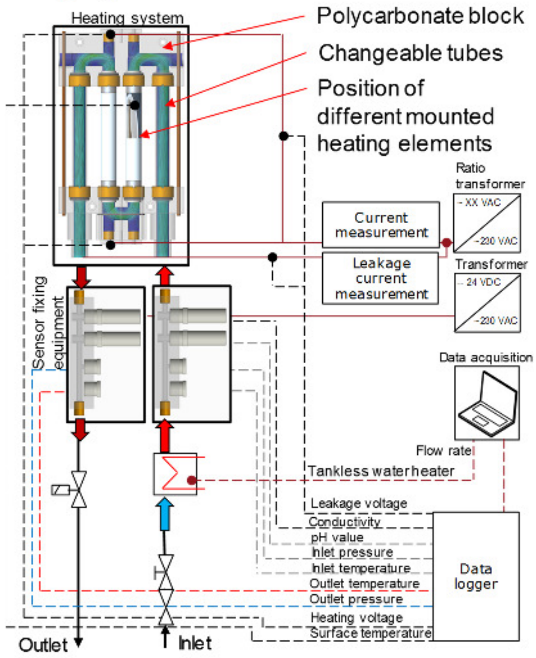

Fig. 4. Schematic of the experimental setup

All process parameters were recorded, including surface temperature, inlet and outlet temperature, electrical voltage, and electrical current. Furthermore, the electrical voltage and electrical current were used to determine the electrical resistance during the period of the test. A variable ratio transformer allowed precise adjustment of the electrical power at the surface. The tankless water heater was used to generate a constant inlet temperature. Furthermore, the electrical conductivity and pH value were measured, too. The core component of the experimental setup is the heating system. The heating device was designed in such a way that all used heating elements could be mounted as bare-wire and tubular heating elements. Moreover, it was also possible to mount the novel heating elements. After the fouling tests, the used tubes with the inserted soiled heating element were dismounted and replaced with a new one. The weight of every heating element was measured prior and subsequent to the execution of each test series. The fouling mass weight was determined based on the weight increase of the heating elements.

The novel heating elements are based on two different coating technologies, namely, thermal spraying and thin film sputtering, which reach heat fluxes higher than 15 W/cm² and an electrical power of approximately 1000 W to heat flowing tap water.

Two heating conductors are used to design conventional and novel heating elements. The most common conductor for conventional electric water heating is nickel-chromium alloy, with a resistivity of 0.00012 Ω·cm. Nickel-chromium is used for conventional and novel heating elements. In this work, one another possible electric conductor is used for water heating, namely, titanium suboxide. Pure titanium suboxide layers have an electric resistivity of 0.04 Ω·cm. The technical data of all used heating elements are presented in Table 3.

Table 3. Technical data of used heating elements

Power P_{el}	Voltage U_R	Current I_R	Resistance R_R	Surface A_s	Heat flux q_{el}
[W]	[V]	[A]	[Ω]	[cm²]	[W/cm²]
Bare-wire heating element with NiCr heating conductor (DW-NiCr)					
1000	115	8.7	13	18.1	56
Tubular heating element with NiCr heating conductor (RHZK-NiCr)					
1000	230	4.3	52	41.0	24
Sputtered thin film heating element with NiCr heating conductor (KF-NiCr-DS)					
1000	230	4.3	52	56.3	18
Thermally sprayed heating element with TiO_x heating conductor (KF-TiO_x-TS)					
1300	230	5.7	40	56.3	23

Thin film heating elements are composed of an Al_2O_3-tube substrate, a thermally insulating Al_2O_3 layer, and a heating layer made of a nickel-chromium alloy (NiCr). The used thermally sprayed multilayer heating elements are composed of a Cu-tube substrate, electrically insulating alumina oxide (Al_2O_3) layers, and a heating layer made of titanium suboxide (TiO_x). Fig. 5 shows the set-up of the novel designed heating elements for the electric water heating.

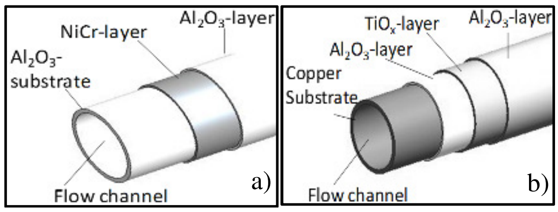

Fig. 5. Set-up of the novel electric heating elements: sputtered thin film heating element (a); thermally sprayed heating element (b)

The surface temperature was measured with a type-K thermocouple to determine the fouling resistance, as shown in Fig. 6a for a novel heating element. The thermocouple was adhered to the surface with a ceramic adhesive with a high thermal conductivity, to have good thermal contact between the heating surface and thermocouple. To determine the heat transfer coefficient and the fouling resistance, it is necessary to calculate the inner temperature of the tube. The inner tube surface temperature is obtained from equation 7:

$$T_{i,s} = T_{a,s} - \frac{U \cdot I}{2 \cdot \pi \cdot l \cdot \lambda_m \cdot \ln\left(\frac{d_a + 2 \cdot t_{iso,i} + 2 \cdot t_{cond} + 2 \cdot t_{iso,a}}{d_i}\right)^{-1}} \qquad (7)$$

As the multilayer is very thin, an averaged thermal conductivity λ_m is used. For both conventional heating elements, the surface temperature is measured directly on the heating element in the water, as shown in Fig 6b for the bare-wire heating element.

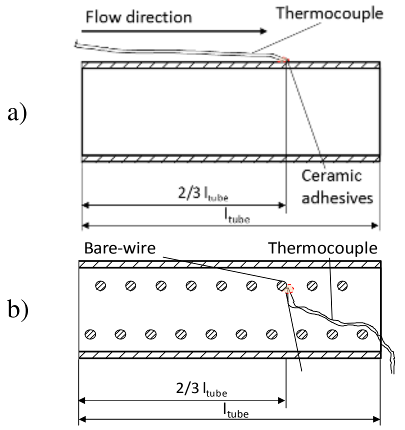

Fig. 6. Schematic of the fabrication of the heating elements with thermocouple: novel heating element (a); bare-wire heating element (b)

Each fouling experiment were conducted with different flowrates of 2 l/min to 4 l/min. The electric heating elements were set to an electrical power of 1000 W at the beginning of each test series. All test series were operated until the electric heating elements failed. Table 4 summarizes these experiments.

Table 4. Parameters of fouling test series

Tests	Heat flux	Liquid temp.	Flowrate	Reynolds number	Outlet pressure	Saturation index
(NE)	$\dot{q}$ [W/cm²]	T_{fl} [°C]	$\dot{V}$ [l/min]	Re [-]	$p_{t,2}$ [bar]	SI [-]
Bare-wire heating element (DW-NiCr)						
1	56	45	2	5250	1	1.32
2	56	45	3	7875	1	1.29
3	56	45	4	10500	1	1.30
Tubular heating element (RHZK-NiCr)						
4	25	45	2	3007	1	2.09
5	25	45	3	4511	1	1.69
6	25	45	4	6014	1	1.70
Sputtered thin film heating element (KF-NiCr-DS)						
7	17.5	45	2	5279	1	1.84
8	17.5	45	3	7919	1	2.30
9	17.5	45	4	10559	1	1.82
Thermally sprayed heating element (KF-TiOx-TS)						
10	18	45	2	5216	1	2.21
11	18	45	3	7824	1	2.25
12	18	45	4	10432	1	2.08

Investigations under clean surface conditions

Different heating elements are prepared for investigation of their durability to crystallization fouling, as explained in previous section. Before these investigations begin, it is necessary to know the heat transfer behavior, the durability, and the technical reliability of novel electric heating elements under clean surface conditions, and compare them with those of the conventional heating elements. With this in mind, the heat transfer coefficient at different flowrates and the dependence of the normalized electrical resistance on heat flux are determined. Moreover, duration tests with dynamic cycles of heating and cooling are conducted with rated loads and overloads for approximately 500 h. The heating cycle lasts 5 min, and the cooling cycle also lasts 5 min. All investigations are performed with the experimental setup shown in Fig. 4. In these investigations, tap water with soft water conditions was used, with saturation indexes lower than zero.

At similar heat fluxes of 15 W/cm², the calculated heat transfer coefficient α is determined under clean surface conditions without deposited fouling layer by the following equation:

$$\alpha = \frac{\dot{q}_{el}}{T_S - T_{fl}} \tag{8}$$

RESULTS AND DISCUSSION

Investigations under clean surface conditions

Fig. 7 compares the flowrate dependence of the heat transfer coefficients of the used heating elements.

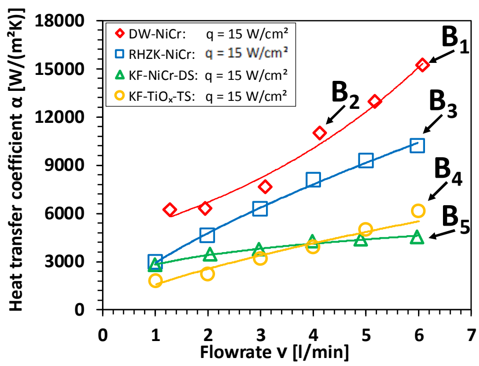

Fig. 7. Heat transfer coefficient of electric heating elements at different flowrates and a heat flux of 15 W/cm²

Bare-wire heating elements reach a maximum heat transfer coefficient of approximately 15000 W/m²K at a flowrate of 6 l/min (B_1). This fact results from the coil flow conditions, the low mass weight of the bare wire, and the low surface temperatures. Additionally, it is observed that with a flowrate of 4 l/min (B_2), the bare-wire heating element begins to swing in the flowing fluid, increasing the turbulence and resulting in an enhancement of the heat transfer coefficient. Tubular heating elements reach heat transfer coefficients of approximately 9000 W/m²K at flowrate of 6 l/min (B_3). The tubular heating element caused a circular ring flow, which resulted in a higher local fluid velocity compared to the novel heating elements. Thus, both novel heating elements reach lower heat transfer coefficients than the conventional elements because of the pipe flow conditions. These elements show heat transfer coefficients of approximately 5000 W/m²K at flowrate of 6 l/min for clean surface conditions, while, the thermally sprayed heating element (B_4) exhibits a higher heat transfer coefficient than the sputtered heating element (B_5).

Fig. 8 shows the dependence of the measured electrical resistance R_{el}^* on the heat flux. If the heat flux is increased over the maximum measured values (M_1, M_2, M_3, M_4), start of boiling at the heating surface can be observed. This phenomenon limits the lifetime of the element.

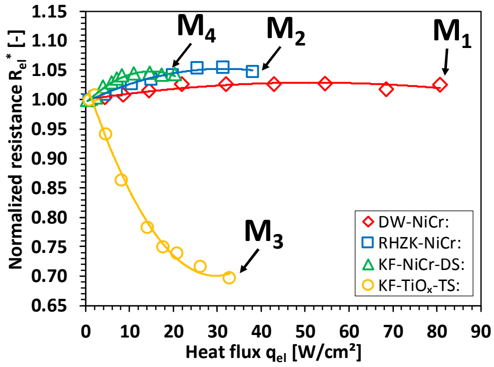

Fig. 8. Normalized electrical resistance of electric heating elements at different heat fluxes and a flowrate at 3 l/min

The results of the investigation of durability behavior of electric heating elements is shown in Fig. 9. All analyzed heating elements show good durability over the testing time of approximately 1000 h. At the end of the durability tests, no change in the normalized electrical resistance was observed for all heating elements.

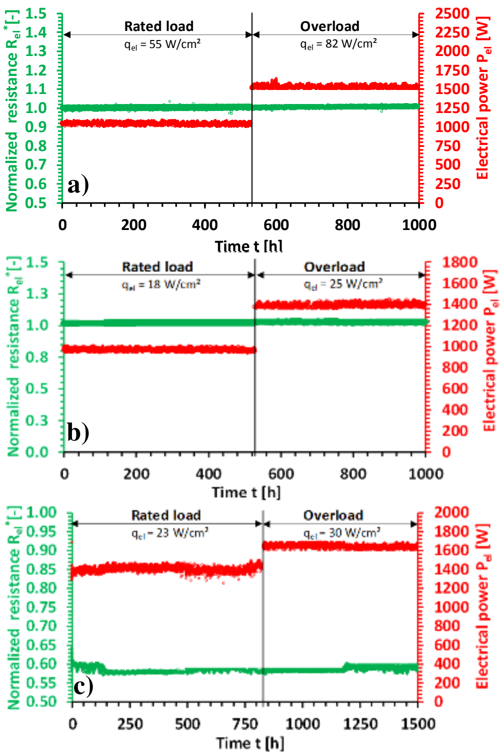

Fig. 9. Duration test under clean surface conditions at a flowrate of 2 l/min and a duration of 1000 h: conventional bare-wire heating element (a); sputtered thin film heating element (b); thermally sprayed heating element (c)

Fouling experiments

In the following subsection, the fouling resistance R_f and the normalized electrical resistance R_{el}^* are analyzed and discussed in terms of their dependence on the flowrates. Furthermore, the induction time, fouling mass weight, and lifetime of the used heating elements are analyzed as a function of the flowrates. Fig. 10 shows a comparison of the fouling resistances and the normalized electrical resistances of different heating elements over the measured lifetime. Fig. 10a shows the fouling curves for all tested heating elements at a flowrate of 2 l/min. The conventional heating elements (NE1 and NE4) and the sputtered thin film heating element (NE7) exhibit a nearly linear crystal growth period until they fail. Only the thermally sprayed heating element shows a sudden increase and sudden decrease in the fouling resistance R_f during the testing period of 58 h to 69 h in test series NE10 (See Fig 10a, P_1). The bare-wire heating element shows slow crystal growth in test series NE1.

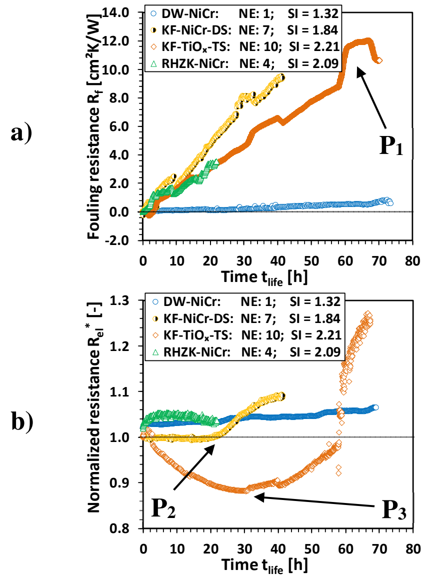

Fig. 10. Comparison of different heating elements at a flowrate of 2 l/min: fouling curves (a); normalized electrical resistance (b)

Fig 10b presents the normalized electrical resistance R_{el}^* for all fouling test series at a flowrate of 2 l/min. The conventional heating elements (NE1 and NE4) show typical electrical resistance R_{el}^* behavior during the heat-up time of NiCr. To begin test series NE 1 and NE4, the normalized electrical resistances R_{el}^* are increased and set to a constant value. After the crystal growth period, the normalized electrical resistance R_{el}^* increases very slowly until the conventional heating elements fail. The tubular heating element failed, because it was not sufficiently cooled, and thus, the heating conductor burned out. In a similar way, the bare-wire heating element failed as well. The sputtered thin film heating element shows a very constant normalized electrical resistance R_{el}^* behavior at the beginning of test series NE7. Although the fouling resistance in test series NE7 increases continuously over time, no degradation of the normalized electrical resistance is observed. After a testing time of 22 h (P_2) the normalized electrical resistance R_{el}^* increases suddenly, because of the deposited crystal layer at the inside of the heating element. In this case, the used ceramic Al_2O_3-substrate experienced micro-cracks at the surface, owing to increased surface temperature, and the heating element failed. Fig. 10b demonstrates that the thermally sprayed heating element at test series NE10 shows interesting behavior for the normalized electrical resistance R_{el}^* in dependence on the time-dependent crystal deposition. From the beginning of the test series to 30 h, the normalized electrical resistance R_{el}^* decreases because of the natural NTC behavior. If the fouling resistance R_f for thermally sprayed heating elements using TiO_x heating conductors increases, the normalized electrical resistance R_{el}^* decreases. After a testing time of 30 h, a turning point (P_3) in the normalized resistance R_{el}^* is observed. The normalized electrical resistance R_{el}^* changed from the NTC to the PTC behavior. This electrical resistance behavior of sprayed TiO_x-conductors shows the beginning of reoxidation. This means that the TiO_x heating layer starts at a surface temperature of 300 °C to uptake oxygen from the environment, as discussed and explained in [2] and [3]. If the heating conductor uptakes oxygen, the normalized electrical resistance increases. Consequently, the heating conductor took more oxygen during the duration of the test, which caused the formation of a hard and brittle heating layer. In test series NE10, a critical turning point (P_3) is reached, which results in the deposition of crystals and, therefore, the continuous increase in the surface temperature over time. After exceeding the critical point (P_3), the heating element is destroyed. Similar fouling durability behavior for the investigated electric heating elements is detected during the execution of all test series with higher flowrates, as presented in Fig. 11.

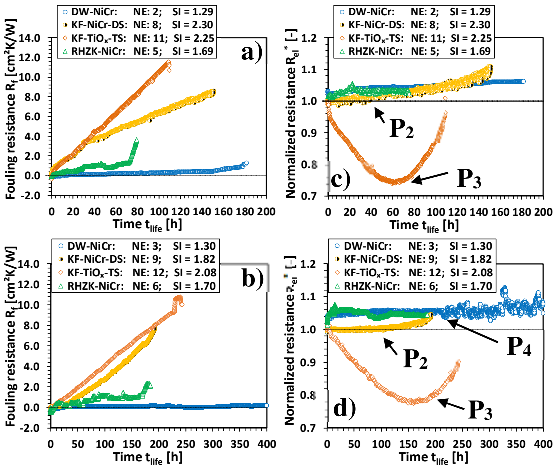

Fig. 11. Comparison of different heating elements: fouling curves (a,b); normalized electrical resistance (c,d). Diagrams (a) and (c) show test series at a flowrate of 3 l/min and diagrams (b) and (d) show test series at a flowrate of 4 l/min

A special electrical resistance behavior (P_4) is observed for bare-wire heating elements in Fig. 11d. In this case, the saw-tooth behavior of the electrical resistance is detected during the layer growth period.

The critical point (P_4) shows that conventional electric heating elements are influenced by fouling before they fail, like novel heating elements (P_2, P_3).

Generally, a reduction in the thermal fouling resistance is observed as the flowrate is increased for all investigated electric heating elements. Furthermore, it is detected a qualitatively similar normalized electric resistance behavior in dependence of the increased flowrate with a higher lifetime. In all investigated cases, the deposited crystals cause a degradation in the normalized electrical resistance.

Fig. 12 shows the determined induction time t_{ind}, in dependence on the flowrates of the investigated heating elements.

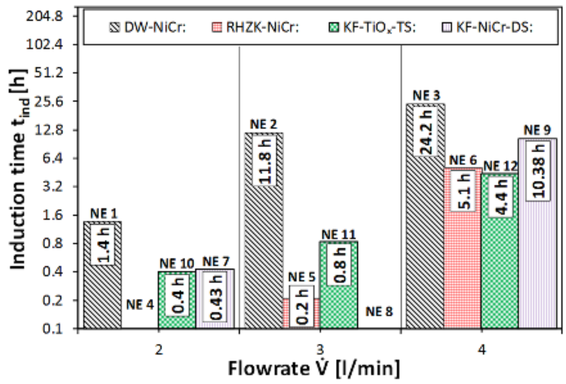

Fig. 12. Comparison of determined induction time of heating elements at different flowrates

The induction time is extended when the flowrate is increased for conventional and thermally sprayed heating elements. Only sputtered thin film heating elements with a ceramic Al_2O_3-heating surface show no induction time for test series NE8. This could be caused by a contaminated heating surface, which led to earlier nucleation and, thus, earlier crystal growth. However, Fig. 12 additionally shows that bare-wire heating elements have the longest induction times. The novel electric heating elements demonstrate higher induction times at low flowrates (2 l/min and 3 l/min) than tubular heating elements do.

Fig. 13 shows the measured fouling mass weight for all heating elements at various flowrates.

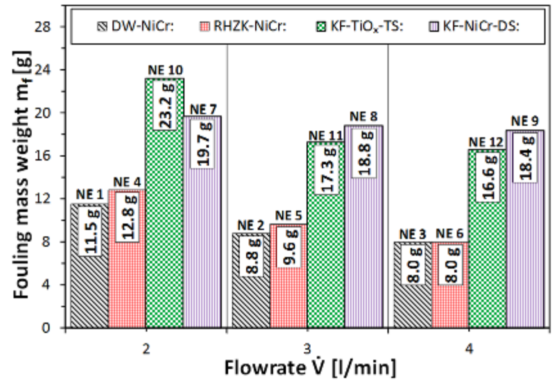

Fig. 13. Comparison of measured fouling mass weight of heating elements at different flowrates

ISBN: 978-0-9984188-1-0; Published online www.heatexchanger-fouling.com

The fouling mass weight is reduced when the flowrate is increased. The deposited fouling mass weight is similar for both conventional heating elements. The amount of deposited fouling for the novel heating elements is nearly twice that of the conventional heating elements. Although more fouling mass weight is deposited for the novel heating elements than for the conventional tubular heating elements, the lifetime of the novel heating elements is longer, as illustrated in Fig. 14.

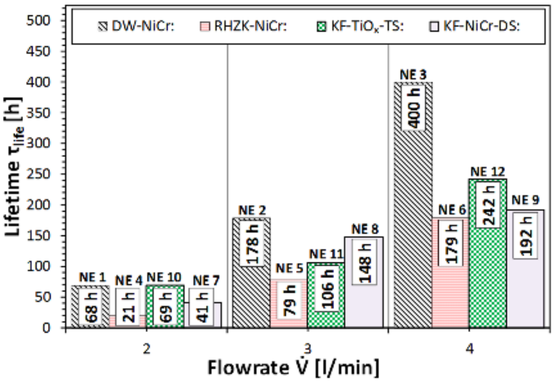

Fig. 14. Comparison of measured lifetime of heating elements at different flowrates

CONCLUSIONS

Conventional and novel electric heating elements were investigated under the influence of crystallization fouling. All presented heating elements operated under clean surface conditions for approximately 1000 h, without any change in the normalized electrical resistance. In the fouling test series, it was shown that all electric heating elements reduced their fouling with increased flowrate. This fact is independent of the heating element geometry. Bare-wire heating elements exhibited the highest induction times and the lowest measured fouling resistances over their lifetime because of their high heat transfer coefficients. The highest fouling resistance values were reached for both novel electric heating elements at the end of their lifetimes. Although, much fouling mass weight was deposited for novel heating elements, their lifetimes were longer than those of conventional tubular heating elements. Moreover, both novel electric heating elements showed higher induction times at low flowrates (2 l/min and 3 l/min) than tubular heating elements. Bare-wire heating elements exhibited the highest fouling durability for each investigated flowrate. In contrast, tubular heating elements showed the lowest lifetimes and, thus, the lowest fouling durability. Furthermore, it was shown that the normalized electrical resistance of the heating conductor was adversely affected by the fouling. It was observed that with an increase in the fouling resistance, the degradation of the normalized electrical resistance began earlier, before the failure of the heating element. This observation was made at both novel electric heating elements and conventional heating elements. Both novel heating elements reached satisfied fouling durability, compared to conventional elements, and could be used in electric water heating.

NOMENCLATURE

A	Surface, m²
d	Diameter, m
k	Overall heat transfer coefficient, W m^{-2} K^{-1}
I	Electrical current, A
l	Length, m
P	Electrical power, W
p	Pressure, bar
$\dot{q}$	Heat flux, W cm^{-2}
R_f	Fouling resistance, cm² K W^{-1}
R_{el}	Electrical resistance, Ω
R_{el}^*	Normalized electrical resistance, dimensionless
SI	Saturation index, dimensionless
T	Temperature, °C
t	Time, s
t	Thickness, m
U	Electrical voltage, V

Greek symbols

α	Heat transfer coefficient, W m^{-2} K
λ	Thermal conductivity, W m^{-1} K^{-1}
ρ	Density, kg m^{-3}
ρ_{el}	Resistivity, Ω·cm

Subscripts

0	Initial clean condition
am	Ambient
a	Outer
cond	Conductor
el	Electrical
el,f	Electrical and fouling
f	Fouling
fl	Fluid
i	Inner
iso	Insulation
m	Average
R	Related value
s	Surface
s,f	Fouled surface
t	Total

REFERENCES

[1] Gusig, L.O.; Schmitz E., *The transient thermal response of conventional and new ceramic electrical heating elements under forced convection,* Industrial furnaces and boilers. European Conference No5, Espinho-Porto, Portugal 2000

[2] Toma F.-L., Scheitz, S., Berger, L.-M., Puschmann, R., Sauchuk, V., Kusnezoff, M., *Development of ceramic heating elements produced by thermal spray technology* International Thermal Spray Conference & Exposition (ITSC 2011)

[3] Scheitz, S., Toma F.-L., Berger, L.-M., Puschmann, R., Sauchuk, V., Kusnezoff, M., *Thermisch gespritzte keramische Schichtheizelemente*, Thermal Spray Bulletin 4 (2011) [2] 88-92

[4] Frey, H., Khan, R. H., *Handbook of thin-film technology*, Springer-Verlag GmbH, 1st ed. 2015

[5] Bach, Fr.-W., Laarmann A., Wenz T., *Modern surface Technology*, WILEY-VCH Verlag GmbH & Co. KGaA, Weinheim 2006

[6] Golan, G., Axelevitch, A., Sigalov B., Gorenstein, B., *Integrated thin film heater-thermocouple systems*, Journal of microelectronics reliability, Volume 43, Issue 3, p. 509-512, 2003

[7] Hwang, J. W., Shin, S. K., Roh, H. J., Lee, S. D., Choa, H. S., *Development of micro-heaters with optimized temperature compensation design for gas sensors*, Journal of sensors, Volume 11, p. 2580-2591, 2011

[8] Bohnet, M., *Fouling of heat transfer surfaces*, Chem. Eng. Techn. 10,2, p. 113-125, 1987

[9] Müller-Steinhagen, H., *Cooling-water fouling in heat exchangers*, Adv. Heat Trans., Vol. 33, pp. 415-496, 1999

[10] Förster, M., Augustin, W., Bohnet, M., *Influence of the adhesion force crystal/heat exchanger surface on fouling mitigation*, Journal of Chemical Engineering and Processing: Process Intensification, Volume 38, Issues 4-6, p. 449-461, 1999

[11] Müller-Steinhagen, H., *Handbook of Heat Exchanger Fouling*, IChemE, Warwickshire, UK 2000

[12] Hirsch, H.; Augustin, W.; Bohnet, M., *Influence of fouling layer shear strength on removal behavior*, Heat Exchanger Fouling and its Mitigation, eds. T.R. Bott et al., New York, p. 201-208, 1999

[13] Wisotzky, F., *Angewandte Grundwasserchemie, Hydrogeologie und hydrogeochemische Modellierung* Springer-Verlag Berlin Heidelberg 2011

[14] Parkhurst, D., Appelo, C.A.J., *Description of Input and Examples for PHREEQC Version 3,* U.S. Geological Survey Techniques and Methods, book 6, chap. A43, 497 p., http://pubs.usgs.gov/tm/06/a43/; 2013